Effect of Cholesterol and Fatty Acids on the Molecular Interactions of Fengycin with *Stratum Corneum* Mimicking Lipid Monolayers

M. Eeman,[†] G. Francius,[‡] Y. F. Dufrêne,[‡] K. Nott,[†] M. Paquot,[†] and M. Deleu*,[†]

Unité de Chimie Biologique Industrielle, Faculté Universitaire des Sciences Agronomiques de Gembloux, Passage des Déportés, 2, B-5030 Gembloux, Belgium, Unité de Chimie des Interfaces, Université Catholique de Louvain, Croix du Sud 2/18, B-1348 Louvain-la-Neuve, Belgium

Received October 16, 2008. Revised Manuscript Received December 23, 2008

The combination of atomic force microscopy (AFM) and the Langmuir trough technique was used in this work to investigate the molecular interactions of fengycin with lipid monolayers constituted of the major lipid classes found in human *stratum corneum* (SC). AFM imaging of spread SC lipids/fengycin monolayers showed that fengycin preferentially partitions into cholesterol-rich phases surrounding 2D domains mainly constituted of ceramide and fatty acid molecules. Penetration experiments of fengycin from the subphase into SC-mimicking monolayers clearly indicated that the lipopeptide insertion at the lipid interface is enhanced in the presence of cholesterol. AFM analysis of mixed SC lipids/fengycin monolayers obtained after lipopeptide penetration revealed that cholesterol strongly interacts with fengycin and undergoes specific molecular interactions with more disordered, loosely packed ceramide molecules. These results highlight the capacity of fengycin to interact with the lipid constituents of the extracellular matrix of SC and, in particular, with cholesterol.

Introduction

The *stratum corneum* (SC), the outermost layer of the skin, protects the body from dehydration and from exposure to different forms of environmental aggression. At the interface between the body and the environment, this layer constitutes only 10% of the entire amount of skin but contributes to over 80% of the cutaneous barrier function.[1] The structure of the SC is unique and can be compared to a two-compartment mortar brick model in which the dead, flattened keratin-filled corneocytes represent the bricks and the extracellular matrix of highly ordered multilamellar lipid sheets plays the role of the mortar.[2] Both the composition and the organization of lipids in the SC are very specific and play an essential role in the skin's protective barrier. Unlike other biological membranes, SC is almost devoid of phospholipids, and its major constituents are ceramides, cholesterol, and long-chain free fatty acids in approximately equimolar proportions.[3−5] Nine different subclasses of ceramides have been identified in human SC.[6−9] The ceramides consist of either a sphingosine, a phytosphingosine, or a 6-hydroxysphingosine base (constituted of an alkyl chain of 16 carbon atoms) to which a nonhydroxy, an α-hydroxy, or an ω-hydroxy chain is linked. The ω-hydroxy ceramide exhibit a longer chain length (between 30 and 34 carbon atoms) than the nonhydroxy and α-hydroxy ceramide (between 16 and 30 carbon atoms) and contain a linoleic acid linked to their ω-hydroxy group.

In addition to the physical barrier provided by the SC lipid matrix, the cutaneous tissue also exhibits a chemical barrier because of the presence of endogenous antimicrobial peptides. These peptides are produced in response to the penetration of the sterile internal environment by invading pathogens. The two major classes of peptides are defensins and cathelicidins. The diversity of peptides found in the skin as well as their role in both healthy and diseased skin were recently reviewed in the literature.[10]

Despite their broad antimicrobial activity, these peptides cannot preserve the skin from all cutaneous damage. The continuous appearance of new bacteria, fungi, parasites, and viruses and the emergence and spread of the antimicrobial resistance phenomenon limit the spectrum of activity of cutaneous antimicrobial peptides. Consequently, new antimicrobial compounds are needed to face the increasing number of infections and the decrease in efficiency of the current endogenous and exogenous antimicrobial agents.

Fengycin produced by several *Bacillus subtilis* strains is a bioactive lipopeptide exhibiting interesting antifungal properties with low hemolytic activity[11,12] that therefore has real potential in the pharmaceutical field and, in particular, dermatology. It is a decapeptide containing a β-hydroxy fatty acid chain (Figure 1A). This lipopeptide class is composed of closely related analogues that differ both in the length of the fatty acid chain (13−17 carbon atoms) and in the nature of the amino acid in position 6 of the peptide moiety (D-Ala or D-Val for fengycin A or fengycin B, respectively). Fengycin includes three amino acid residues that can be protonated or deprotonated according to pH. At neutral pH, it exhibits two negative charges (glutamic acid residues) and one positive charge (ornithine residue), which affect its conformation and play an important role in its

* Corresponding author. Phone: (32) 81 62 22 32. Fax: (32) 81 62 22 31. E-mail: deleu.m@fsagx.ac.be.

[†] Faculté Universitaire des Sciences Agronomiques de Gembloux.

[‡] Université Catholique de Louvain.

(1) Pouillot, A.; Dayan, N.; Polla, A. S.; Polla, L. L.; Polla, B. S. *J. Cosmet. Dermatol.* **2008**, *7*, 143.

(2) Elias, P. M. *J. Invest. Dermatol.* **1983**, *80*, 44s–49s.

(3) Downing, D. T.; Stewart, M. E.; Wertz, P. W.; Colton, S. W.; Abraham, W.; Strauss, J. S. *J. Invest. Dermatol.* **1987**, *88*, 2s.

(4) Law, S.; Wertz, P. W.; Swartzendruber, D. C.; Squier, C. A. *Arch. Oral Biol.* **1995**, *40*, 1085.

(5) Wertz, P. W.; van den Bergh, B. *Chem. Phys. Lipids* **1998**, *91*, 85.

(6) Wertz, P. W.; Miethke, M. C.; Long, S. A.; Strauss, J. S.; Downing, D. T. *J. Invest. Dermatol.* **1985**, *84*, 410.

(7) Robson, K. J.; Stewart, M. E.; Michelsen, S.; Lazo, N. D.; Downing, D. T. *J. Lipid Res.* **1994**, *35*, 2060.

(8) Stewart, M. E.; Downing, D. T. *J. Lipid Res.* **1999**, *4*, 1434.

(9) Ponec, M.; Weerheim, A.; Lankhorst, P.; Wertz, P. *J. Invest. Dermatol.* **2003**, *120*, 581.

(10) Namjoshi, S.; Caccetta, R.; Benson, H. A. E. *J. Pharm. Res.* **2008**, *97*, 2524.

(11) Vanittanakom, N.; Loeffler, W.; Koch, U.; Jung, G. *J. Antibiot.* **1986**, *39*, 888.

(12) Schneider, J.; Taraz, K.; Budzikiewicz, H.; Deleu, M.; Thonart, P.; Jacques, P. *Z. Naturforsch.* **1999**, *54c*, 859.

10.1021/la803439n CCC: $40.75
Published on Web 02/03/2009

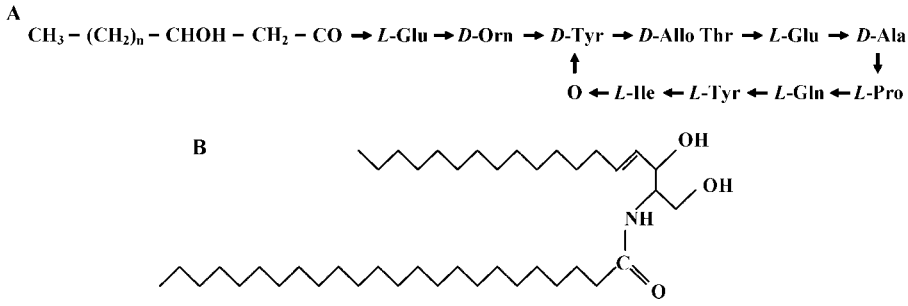

Figure 1. Primary structure of (A) fengycin A ($n = 12$ for fengycin with a β-hydroxy fatty acid chain of 16 carbon atoms) and (B) C_{24}-ceramide 2 (*N*-lignoceroyl-D-sphingosine).

intermolecular interactions.[13] In the current work, the most abundant fengycin analogue produced by the *Bacillus subtilis* S499 strain is used. This specific variant comprises a β-hydroxy fatty acid chain of 16 carbon atoms (fengycin A C_{16}).

The molecular interactions between fengycin A C_{16} and SC models have already been investigated in one of our previous studies.[14] The model used to mimic the SC lipid composition was a lipid monolayer constituted only of ceramides, one of the three main lipid classes found in human SC. The combination of atomic force microscopy (AFM) and surface pressure−area isotherms leads to the conclusion that both of the environmental conditions (temperature and pH) and the fengycin concentration influence the tendency of ceramide to form 2D domains. From these results, we presumed that the biological activity of the lipopeptide may be linked to its capacity to modulate the ceramide properties (molecular organization, phase separation, and fusogenic activity) in the cutaneous membrane.

Because ceramides do not represent the only lipid class in SC, the present work aims at determining the influence of cholesterol and free fatty acids, the two other major lipid constituents of SC, on the molecular interactions of the specific fengycin A C_{16} analogue with SC-mimicking lipid monolayers. A C_{24}-ceramide 2 (Figure 1B) was incorporated into the SC models because ceramides of type 2 are the most prevalent in epidermal SC and the fatty acid linked to their sphingosine base exhibits a length distribution ranging from 16 to 30 carbon atoms, with 24 (C_{24}) and 26 (C_{26}) carbon chain lengths being the most abundant.[3,4,15,16] Lignoceric acid (C_{24}-fatty acid) was chosen to represent the free fatty acid composition of SC in the SC models because it is, with the C_{22}-fatty acid, the most abundant free fatty acid in intact SC.[17−19] To study the interfacial properties of fengycin incorporated into or spread with SC lipid monolayers, AFM is combined with the Langmuir trough technique. Molecular interactions are evaluated by analyzing domain formation, step height, and friction contrast from the AFM images as well as surface pressure variation and exclusion pressure from the penetration kinetics.

The objective of this article is to describe the first step toward investigating the potential diffusion of fengycin through the extracellular lipid matrix of the SC. It is imperative to determine if a compound that exhibits specific antimicrobial activity is able to reach the target area where the microbes proliferate and induce infections. In the particular case of skin diseases, most of the microbes are localized in the epidermis. For example, *Candida albicans*, which is known to proliferate in acidic environment, is mainly located in the upper layers of the epidermis where it is responsible for fungal cutaneous infections. The investigation of molecular interactions between fengycin and the major SC lipids, which mainly govern the ability of a drug to diffuse through the uppermost layer of the skin, is a primary step in the determination of the potential of fengycin to overcome the physical barrier of SC.

Materials and Methods

Chemicals. Fengycin A with a β-hydroxy fatty acid chain of 16 carbon atoms (molecular weight, 1462.8 g/mol) (Figure 1A) was produced as described previously.[20,21] Isolation of this molecule from crude fengycins was performed by preparative reverse-phase chromatography. The identification and verification of the purity were made by amino acid analysis,[22] analytical RP-HPLC, and MALDI-TOF mass spectrometry (Ultraflex TOF, Bruckner, Karlsruhe, Germany). The HPLC-UV (205 and 214 nm) purity of the fengycin molecules was always higher than 95%.

N-Lignoceroyl-D-sphingosine (C_{24}Cer2) (Figure 1B) and cholest-5-en-3β-ol (Chol) were purchased from Avanti Polar Lipids (Alabaster, AL). Lignoceric acid (C_{24}FA) was purchased from Sigma-Aldrich (St. Louis, MO). All of these chemicals were used without further purification.

The buffer used in this work was a phosphate-buffered saline (abbreviated PBS buffer) and was constituted of $NaH_2PO_4 \cdot H_2O$/Na_2HPO_4/NaCl 20/20/150 mM. The adjustment of the pH (pH 7.4) was done by adding an adequate amount of 7.5 M NaOH.

Monolayer Studies. For isotherm experiments, lipid monolayers were prepared at 32 ± 0.2 °C with an automated LB system (KSV minitrough, KSV instruments Ltd., Helsinki, Finland). Fengycin as well as the three lipids used to mimic the lipid composition of SC (C_{24}Cer2, Chol, and C_{24}FA) were dissolved in chloroform/methanol (2:1 v/v) to give a concentration of 1 mM. Pure solutions as well as 0.25:0.75 molar mixtures of fengycin and SC models were spread on a PBS subphase. After a waiting time of 15 min allowing solvent evaporation and spreading of the molecules, the monolayers were compressed at a rate of 10 mm/min. The surface pressure of the lipid monolayer was measured using a platinum plate with an accuracy of 0.1 mN/m. The difference between the molecular areas of two independent sets of measurements was less than 5%. To analyze their nanoscale interfacial behavior by AFM, the mixed SC lipids/fengycin monolayers were transferred onto a freshly cleaved mica sheet (width, 10 mm; height, 15 mm) by raising the mica support

(13) Eeman, M.; Pegado, L.; Dufrene, Y.; Paquot, M.; Deleu, M. *J. Colloid Interface Sci.* **2009**, *329*, 253.
(14) Eeman, M.; Deleu, M.; Paquot, M.; Thonart, P.; Dufrene, Y. *Langmuir* **2005**, *21*, 2505.
(15) Swartzendruber, D. C.; Kitko, D. J.; Wertz, P. W.; Downing, D. T. *Arch. Dermatol. Res.* **1988**, *280*, 424.
(16) Bouwstra, J. A.; Gooris, G. S.; Cheng, K.; Weerheim, A.; Bras, W.; Ponec, M. *J. Lipid Res.* **1996**, *37*, 999.
(17) Lampe, M. A.; Burlingame, A. L.; Whitney, J.; Williams, M. L.; Brown, B. E.; Roitman, E.; Elias, P. M. *J. Lipid Res.* **1983**, *24*, 120.
(18) Wertz, P. W.; Downing, D. T. In *Physiology, Biochemistry and Molecular Biology of the Skin*; Goldsmith, L. A., Ed.; Oxford University Press: Oxford, U.K., 1991; pp 205−235.
(19) Norlén, L.; Nicander, I.; Lundsjö, A.; Cronholm, T.; Forslind, B. *Arch. Dermatol. Res.* **1998**, *290*, 508.
(20) Jacques, P.; Hbid, C.; Destain, J.; Razafindralambo, H.; Paquot, M.; De Pauw, E.; Thonart, P. *Appl. Biochem. Biotechnol.* **1999**, *77*−*79*, 223.
(21) Razafindralambo, H.; Paquot, M.; Hbid, C.; Jacques, P.; Thonart, P. *J. Chromatogr.* **1993**, *639*, 81.
(22) Moore, S.; Stein, W. *J. Biol. Chem.* **1951**, *192*, 663.

vertically through the air−water interface at a speed of 10 mm/min. The transfer ratios (i.e., ratio of the lipid film area deposited onto the surface of the support)[23] were all close to 1, confirming that AFM images were representative of the spread monolayer. The fraction γ of the surface occupied by a component i in mixed monolayers constituted of n different components has been calculated as follows

$$\gamma = \frac{X_i A_i}{\sum_{i=1}^{n} X_i A_i} \quad (1)$$

where X_i and A_i are the molar ratio of constituent i in the mixture and the mean molecular area occupied by component i at a defined surface pressure Π in its pure monolayer, respectively.

For adsorption experiments, the same system was used. The adsorption area (75×160 mm^2) was delimited by two symmetrical barriers, which were kept immobile during all of the measurement at the edges of the trough, and corresponded to the same effective area as the one used in the penetration experiments. The injection of fengycin molecules, solubilized in dimethylsulfoxide (DMSO) (99.90% ACS reagent, Sigma), in the subphase (final concentration of 5.0×10^{-7} M) was done by using a Hamilton syringe and two homemade devices allowing the injection of fengycin without disturbing the air−water interface. These devices were placed at two fixed positions on the trough to ensure a reproducible injection process. Furthermore, during the entire duration of the experiment, the subphase was stirred using two cylindrical micromagnetic rods (8×1.5 mm^2) and two electronic stirrer heads located beneath the trough (model 300, Rank Brothers, Bottisham, U.K.). An autoreversing mode with slow acceleration and a stirring speed of 100 rpm was selected. After the injection of fengycin, the increase in surface pressure was recorded.

For the penetration experiments, lipid monolayers were prepared with the same LB system as above. The defined initial surface pressure of these monolayers was obtained by spreading a precise volume of SC-mimicking model solutions prepared in chloroform/methanol (2:1 v/v). As soon as the initial surface pressure was stabilized (~20 min), fengycin, solubilized in DMSO, was injected into the subphase to a final concentration of 5.0×10^{-7} M using the same injection setup as described above. Because the critical micelle concentration of fengycin is 1.2 ± 0.1 μM under the conditions used in the current work (PBS buffer, pH 7.4, 32 °C; unpublished results), it can be assumed that at a concentration of 5.0×10^{-7} M, fengycin does not self-assemble and exists mainly as monomers within the subphase. When the surface pressure reached a maximal stable value, the monolayer was deposited onto a mica support (via the same procedure as for the isotherm experiments) and analyzed by AFM. For the penetration experiments, the transfer ratios were all also close to 1, confirming that AFM images were representative of the SC lipid monolayers after the penetration of fengycin. Pure DMSO injections into the subphase did not modify the initial surface pressure of the SC-mimicking monolayers.

AFM Measurements. AFM measurements on the LB-supported monolayers were performed in air and at room temperature (20 °C) using a commercial optical lever microscope (Nanoscope III, Digital Instruments, Santa Barbara, CA). Topographic images (512 pixels $\times$ 512 pixels) were taken in constant-deflection mode using oxide-sharpened microfabricated Si_3N_4 cantilevers (Park Scientific Instruments, Mountain View, CA) with a typical curvature radius of 20 nm and spring constants of 0.01 and 0.03 N/m. The applied force was kept as low as possible during imaging, and the scan rate was 3 Hz. Images were obtained from two independent samples and from three to five different areas on each sample. Thickness variations were determined from section analysis of five topographic images, avoiding shadowed areas due to flattening effects. Surface percentages occupied by lower and higher domains in AFM topographic images were obtained using the WSxM 4.0 Develop 11.4 software.[24]

Results and Discussion

Four different lipid compositions were used (pure ceramide, ceramide/cholesterol 3/1, ceramide/cholesterol 2/1, and ceramide/cholesterol/fatty acid 1/1/1) to investigate the interfacial properties of fengycin and its molecular interactions with the main lipid classes of SC. Two kinds of experiments were conducted. In the first type (isotherm experiments), fengycin and SC models were mixed and spread at the interface of a PBS buffer subphase at 32 °C and pH 7.4. In the second kind of experiment (penetration experiments), fengycin was injected into a PBS subphase covered with a lipid monolayer consisting of one of the four SC models. For both types of experiments, AFM was used to record topographic and friction images of mixed SC models/fengycin monolayers transferred onto a mica support by the Langmuir−Blodgett (LB) technique.

Interfacial Properties of Spread SC Lipids/Fengycin Monolayers. Figure 2A presents the surface pressure−area $\Pi-A$ isotherms of pure C_{24}-ceramide 2, pure cholesterol, and pure C_{24}-fatty acid monolayers.

The shape and steepness of the $\Pi-A$ isotherm of pure ceramide show that the molecules exclusively form a very condensed monolayer at the air−water interface. No transition from the liquid-expanded to the liquid-condensed state can be observed. Such interfacial behavior was already reported for another subclass of ceramide (ceramide 3) that is composed of a phytosphingosine base.[25,26] The shape of the $\Pi-A$ isotherm of pure C_{24}-ceramide 2 is also similar to the one that we have reported for a ceramide from the same subclass (composed of a sphingosine base) but with a much smaller alkyl chain length (16 vs 24 carbon atoms).[14] However, the mean molecular area of the C_{24}-ceramide is slightly higher than the area occupied by the C_{16}-ceramide. (At 20 mN/m, the mean molecular areas are 38 and 44 Å^2 for C_{16}- and C_{24}-ceramide, respectively.) This difference may arise from the nature of the subphase. Under the present conditions, two additional ions, namely, phosphate ions HPO_4^{2-} and $H_2PO_4^-$, are found in the subphase. Because of their large size, these phosphate anions may induce steric effects in the interfacial film and therefore slightly expand the lipid monolayer.[27]

The steep slope of the $\Pi-A$ isotherm of pure cholesterol indicates that this lipid exists only in a very condensed state up to the monolayer collapse. A mean molecular area of 40 Å^2 at 20 mN/m is in agreement with other values reported in the literature.[25,26,28]

The area occupied by the lignoceric fatty acid at 20 mN/m (A = 21 Å^2/molecule) is similar to the one found by Ekelund and colleagues.[29] However, the shape of its $\Pi-A$ isotherm is slightly different. These authors reported a clear liquid condensed phase to a solid-phase transition at a surface pressure of about 12 mN/m. Under the specific conditions used in this work, which are closer to physiological ones, the $\Pi-A$ isotherm of the lignoceric acid exhibits only a small kink around 35 mN/m. This kink

(23) Silvestro, L.; Axelsen, P. H. *Chem. Phys. Lipids* **1998**, *96*, 69.

(24) Horcas, I.; Fernandez, R.; Gomez-Rodriguez, J. M.; Colchero, J.; Gomez-Herrero, J.; Baro, A. M. *Rev. Sci. Instrum.* **2007**, *78*, 013705.

(25) ten Grotenhuis, E.; Demel, R. A.; Ponec, M.; Boer, D. R.; van Miltenburg, J. C.; Bouwstra, J. A. *Biophys. J.* **1996**, *71*, 1389.

(26) Sparr, E.; Eriksson, L.; Bouwstra, J. A.; Ekelund, K. *Langmuir* **2001**, *17*, 164.

(27) Boury, F.; Gautier, J.-C.; Bouligand, Y.; Proust, J.-E. *Colloids Surf., B* **2001**, *20*, 219.

(28) Flach, C. R.; Mendelsohn, R.; Rerek, M. E.; Moore, D. J. *J. Phys. Chem. B* **2000**, *104*, 2159.

(29) Ekelund, K.; Sparr, E.; Engblom, J.; Wennerström, H.; Engström, S. *Langmuir* **1999**, *15*, 6946–6949.

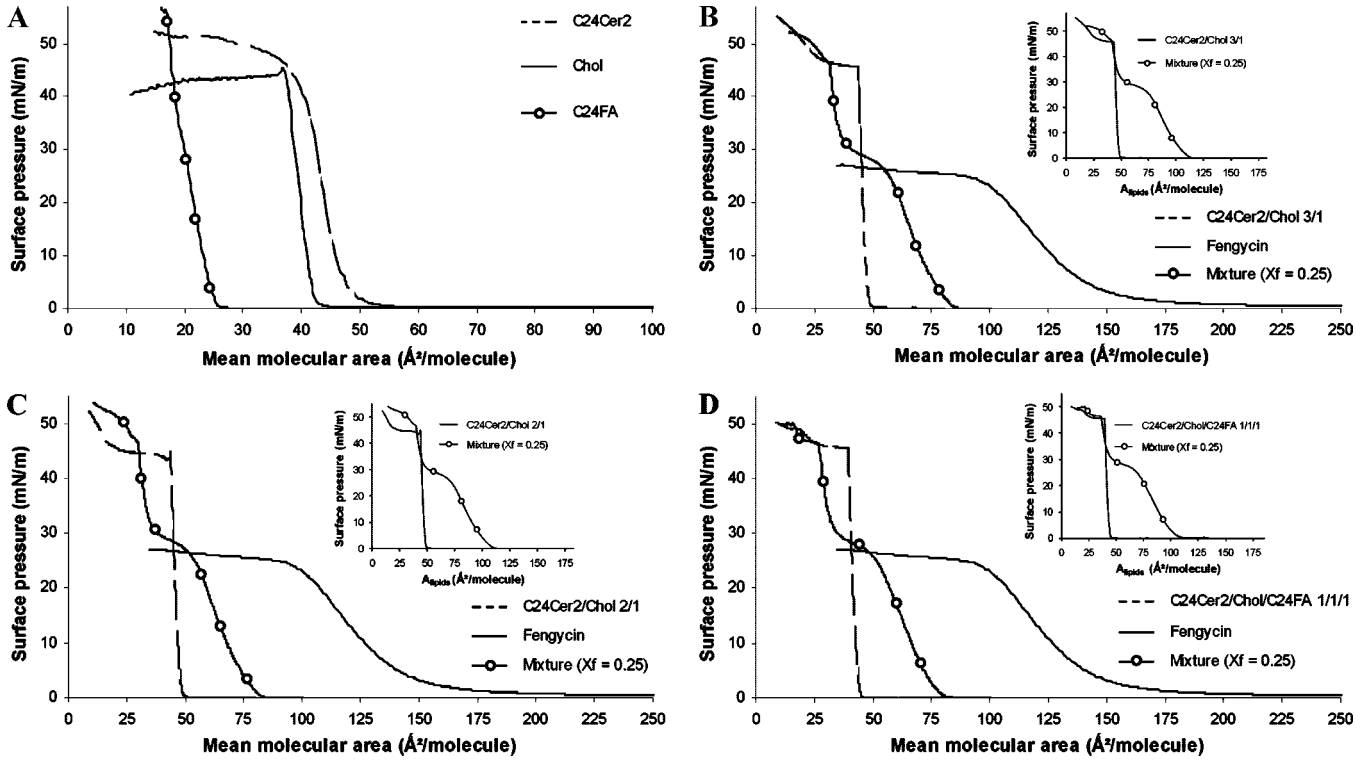

Figure 2. Surface pressure−area (Π−*A*) isotherms, at the air−water interface, of (A) pure ceramide, pure cholesterol, and pure fatty acid monolayers; (B) a pure fengycin monolayer, a mixed ceramide/cholesterol (molar ratio 3/1) monolayer, and a mixed ceramide/cholesterol (molar ratio 3/1) monolayer containing a 0.25 fengycin molar ratio; (C) a pure fengycin monolayer, a mixed ceramide/cholesterol (molar ratio 2/1) monolayer, and a mixed ceramide/cholesterol (molar ratio 2/1) monolayer containing a 0.25 fengycin molar ratio; and (D) a pure fengycin monolayer, a mixed ceramide/cholesterol/fatty acid (molar ratio 1/1/1) monolayer, and a mixed ceramide/cholesterol/fatty acid (molar ratio 1/1/1) monolayer containing a 0.25 fengycin molar ratio. (Inset in B−D) The same isotherms as the ones presented in the corresponding graphs but plotted as a function of the mean molecular area of the lipid components alone (A_{lipids}). Monolayers were recorded at 32 °C with a PBS subphase at pH 7.4.

probably corresponds to the onset of the solid phase because it can be assumed that increasing the temperature from 19 °C (subphase temperature used by Ekelund et al.)[29] to 32 °C (subphase temperature in this study) modifies the ordering of the fatty acid chain and is responsible for the apparition of the solid phase only at higher surface pressure.

These three pure lipid monolayers exhibit a relatively low compressibility as suggested by their steep slope and their two-dimensional compressibility coefficient C_s at 20 mN/m (C_s = 4.7, 2.8, and 7.3 m/N for ceramide, cholesterol, and fatty acid, respectively).

The addition of cholesterol to a ceramide monolayer significantly affects its Π−*A* isotherm (Figure 2B,C). Indeed, the rounded shape observed at low and high surface pressures of the pure ceramide Π−*A* isotherm (Figure 2A), which indicates a molecular rearrangement at the air−water interface,[26] disappears in the presence of cholesterol (for cholesterol-to-ceramide molar ratios of 0.25 and 0.33). The shape of the Π−*A* isotherm of the ceramide/cholesterol mixture closely resembles that of pure cholesterol, but it is displaced to higher molecular areas (A = 46 Å^2/molecule for both ceramide/cholesterol 3/1 and 2/1 monolayers at 20 mN/m) that are close to the mean molecular area of the pure ceramide monolayer. Furthermore, the compressibility of mixed ceramide−cholesterol monolayers is lower than the compressibilities of both the pure ceramide and the pure cholesterol monolayers (C_s = 1.8 and 1.9 m/N at 20 mN/m for mixed ceramide/cholesterol 3/1 and 2/1 monolayers at 20 mN/m, respectively).

The further addition of fatty acid to a mixed ceramide/cholesterol monolayer does not significantly affect either the shape or the 2D compressibility of the Π−*A* isotherm (C_s = 2.1 m/N for mixed ceramide/cholesterol/fatty acid 1/1/1 monolayers at 20 mN/m) (Figure 2D). However, it induces a shift in the Π−*A* isotherm to smaller mean molecular areas (A = 41 Å^2/molecule for the ceramide/cholesterol/fatty acid 1/1/1 monolayer at 20 mN/m). All of these results indicate that cholesterol (>33 mol %) strongly modulates the interfacial 2D organization of both ceramide and fatty acid molecules in SC-mimicking monolayers. Similar effects of cholesterol on both the shape and the 2D compressibility of Π−*A* isotherms of other lipids characteristic of biological membranes have also been reported in the literature.[30−32]

As observed previously,[13,14] the Π−*A* isotherm of the pure fengycin exhibits a sigmoidal shape (Figure 2B−D). At large molecular areas, low and relatively constant surface pressure is recorded, corresponding to a gaseous state. Further compression of the fengycin monolayer induces a progressive increase in surface pressure, indicating the appearance of a liquid-expanded state that is characterized by a certain degree of cooperative interaction between the molecules at the interface. This increase in surface pressure is followed by a final plateau of constant surface pressure. No sharp increase in surface pressure is observed even at very low areas per molecule, indicating that the fengycin monolayer cannot adopt a liquid-condensed state even under high compression.[13] The final plateau at constant surface pressure most likely results from a progressive desorption of the lipopeptide from the air−water interface.[13]

(30) Mozaffary, H. *Thin Solid Films* **1994**, *244*, 874.
(31) Gong, K.; Feng, S.-S.; Go, M. L.; Soew, P. H. *Colloids Surf., A* **2002**, *207*, 113.

The addition of fengycin (at a fengycin molar ratio X_f of 0.25) to the one- (data not shown), two-, and three-lipid component SC models gives rise to very similar $\Pi-A$ isotherms (Figure 2B−D). Whatever the composition and the lipid proportion of the SC-mimicking monolayers, the $\Pi-A$ isotherms obtained in the presence of fengycin show the existence of two states, a fluid-like and a solid-like, as well as a phase transition between these two states. This transition occurs at the surface pressure at which the final plateau of the pure fengycin isotherm (about 25 mN/m) starts. After the transition, the isotherms of the mixed SC lipids/fengycin monolayers present a steep slope similar to that of the isotherms of the SC lipid mixtures but at lower values of the mean molecular area. If the same isotherms are plotted as a function of the mean molecular area of the lipid components alone (A_{lipids} calculated by dividing the area of the monolayer by the total number of SC lipid molecules present at the air−water interface), then the isotherms of the mixed SC lipid/fengycin monolayers now overlay the isotherms of the SC lipid mixtures in the region after the transition (inset in Figure 2B−D). This indicates that the transition in the mixed SC lipid/fengycin isotherms is related to fengycin squeeze out and that the solid-like part of these curves is mainly due to the SC lipids. As also suggested for mixed dipalmitoylphosphatidylcholine/fengycin monolayers in one of our recent study,[13] fengycin molecules are thus progressively squeezed out of the mixed monolayers when the surface pressure is increased, without carrying lipid molecules out of the monolayer.

SC-mimicking monolayers with and without lipopeptide were transferred onto the mica sheet by the LB technique and analyzed by AFM to investigate the effect of fengycin on their nanoscale properties.

Figure 3 presents AFM topographic images obtained for the SC-mimicking models in the absence of fengycin. The addition of cholesterol to a pure ceramide monolayer induces the formation of phase separation at the air−water interface: larger and smaller domains without a well-defined shape are floating on a continuous matrix that is found at a lower level (step height of about 1.0 nm, see Table 1; Figure 3A,B). Considering the surface coverage S of the lower phase in the AFM images ($S = 24-27\%$ and $30-35\%$ in Figure 3A,B, respectively) and the calculated fraction γ (eq 1) of the surface occupied by cholesterol in the mixed monolayers ($\gamma = 23$ and 31% for monolayers of ceramide/cholesterol 3/1 and 2/1, respectively), the higher domains can be attributed to ceramide-rich aggregates whereas the surrounding phase is essentially constituted of cholesterol. The absence of strong miscibility between both components at the air−water interface has been pointed out in previous studies.[25,26,29] However, the nanoscale organization and, in particular, the shape and the size of ceramide domains within the cholesterol environment found in these earlier studies strongly differ from the phase separation shown in the current work. Indeed, they have shown that ceramide molecules form small interconnected rectangular domains that are segregated from the cholesterol-rich phase with a step height between the two phases of about 0.6−0.8 nm. Such a discrepancy in the nanoscale organization of mixed cholesterol/ceramide monolayers may be due to differences in experimental parameters (nature and temperature of the aqueous subphase as well as the surface pressure used for the LB technique), which have been shown to affect the lipid packing within the ceramide domains and, consequently, the shape of these domains.[14] However, in this case, it is most likely that the discrepancy in the nanoscale organization mainly arises from the type of ceramides mixed with cholesterol in the monolayers. We used a sphingosine subclass of ceramides (C_{24}Cer 2) whereas the other studies were performed using a phytosphingosine subclass of ceramides (C_{24}Cer 3). Compared to the former subclass, the latter does not possess a trans double bond in position 4,5 of the base chain but exhibits an additional hydroxyl group in position 4. This change in the molecular structure of ceramides modifies the driving force for their molecular self-assembly and consequently affects the shape of the molecular aggregates. As reported in the literature,[33] the driving force for the self-assembly of sphingosines is interactions between the hydrocarbon chains, resulting in the formation of very dense ceramide domains with an orthorhombic lateral chain packing, whereas the aggregation of phytosphingosines is driven by headgroup hydrogen bonding. The presence of hydrogen bonding between phytosphingosine headgroups and the hydroxyl group of cholesterol probably promotes better miscibility of both components at the air−water interface by reducing the line tension along the ceramide domain boundaries.

Raising the cholesterol content in mixed ceramide/cholesterol monolayers (from 3/1 to 2/1 for parts A and B of Figure 3, respectively) slightly increases the interfacial perimeter between the cholesterol-rich and ceramide-rich phases as observed by the more convoluted boundaries of the ceramide domains in the case of a 33 mol % containing monolayer (Figure 3B). The decrease in the line tension along the ceramide domains as a result of the higher cholesterol content is also at the origin of the partial disruption of the large ceramide domains and consequently an increase in the number of smaller ceramide aggregates floating on the cholesterol-rich matrix. A stronger dispersion of ceramide domains by increasing the cholesterol content in mixed monolayers has also been found in LB-supported films of human SC lipids.[34]

The addition of fatty acid to yield an equimolar mixture of ceramide, cholesterol, and fatty acid further affects the nanoscale organization of the SC models. The AFM topographic image of a mixed ceramide/cholesterol/fatty acid 1/1/1 monolayer (Figure 3C) reveals phase separation with a step height (about 1.3 nm) that is slightly higher than the step height values observed in the absence of fatty acid (Table 1). Because of the matching of the alkyl chains of the ceramide and the fatty acid, we assume that these two components are miscible and segregate together from the cholesterol-rich phase. The partitioning of ceramide and fatty acid in the same domains is confirmed by a comparison of the surface coverage. The higher phase occupies a similar percentage ($S = 58-63\%$) to the calculated fraction γ of the surface occupied by ceramide and fatty acid molecules in the mixed ceramide/cholesterol/fatty acid 1/1/1 monolayers ($\gamma = 42 + 20\%$ for ceramide and fatty acid, respectively). Such miscibility between ceramide and fatty acid was already observed in another study in which a C_{24}-phytosphingosine was used to mimic the ceramide composition of the SC.[26] The step height observed by these authors between the ceramide/fatty acid domains and the cholesterol-rich matrix is about 1.2 nm, which is in good agreement with our results. All of these data show that, whatever the nature of the headgroup of ceramides (sphingosine vs phytosphingosine), fatty acid molecules increase both the step height between the ceramide domains and the cholesterol-rich environment and the line tension along the ceramide aggregates. The effect of long-chain fatty acids on the nanoscale organization in mixed ceramide/cholesterol monolayers can be explained as follows: because of their preferential incorporation into the ceramide domains and

(32) Gzyl-Malcher, B.; Handzlik, J.; Nowak-Stepniowska, A. *Colloids Surf., A* **2008**, *321*, 52.

(33) Rerek, M. E.; Chen, H.-C.; Markovic, B.; Van Wyck, D.; Garidel, P.; Mendelsohn, R.; Moore, D. J. *J. Phys. Chem. B* **2001**, *105*, 9355.

(34) Norlén, L.; Plasencia Gil, I.; Simonsen, A.; Descouts, P. *J. Struct. Biol.* **2007**, *158*, 386.

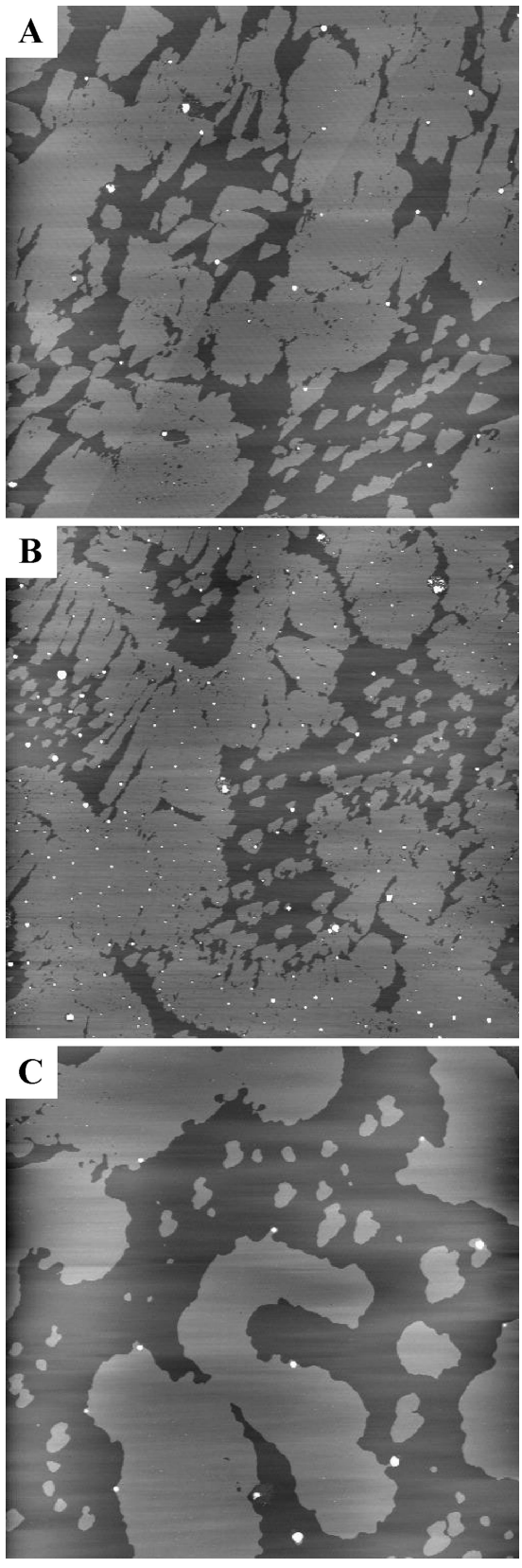

Figure 3. Effect of the presence of cholesterol and C_{24}-fatty acid on the organization of SC-mimicking lipid monolayers. AFM height images (size, 20 μm × 20 μm; z range, 5 nm) obtained for (A) mixed ceramide/cholesterol (molar ratio 3/1) monolayers; (B) mixed ceramide/cholesterol (molar ratio 2/1) monolayers; and (C) mixed ceramide/cholesterol/fatty acid (molar ratio 1/1/1) monolayers prepared on a PBS subphase at pH 7.4 and 32 °C. The surface pressure used for the LB transfer is 20 mN/m. Lighter levels in the images correspond to higher heights. Duplicate experiments using independent preparations yielded similar results.

Table 1. Step Height between the Thicker and the Thinner Phases Observed in the AFM Topography Images[a]

SC-mimicking lipid monolayer	without fengycin[b]	spread with fengycin[c]	after penetration of fengycin[d]
C24Cer2		1.2	1.2
C24Cer2/Chol 3/1	1.1	1.0	0.6 and 1.0
C24Cer2/Chol 2/1	1.0	0.7	0.7 and 1.1
C24Cer2/Chol/C24FA 1/1/1	1.3	0.9	1.0 and 1.5

[a] Step height Δh (±0.1 nm) between the thicker and thinner phases obtained from three cross-sections from three different AFM topography images. When two values are reported, the first one corresponds to the step height between the thinner and the intermediate phases, and the second one corresponds to the step height between the thinner and thicker phases. [b] Step height obtained for monolayers constituted of only SC lipids. [c] Step height obtained for spread fengycin/SC lipid monolayers. The fengycin molar ratio (X_f) in the mixtures is 0.25. [d] Step height obtained for fengycin/SC lipid monolayers obtained after the penetration of fengycin into the interfacial film initially constituted of SC lipids.

not in the cholesterol-rich surrounding phase, the fatty acid molecules increase the lipid density and the lipid packing within the ceramide aggregates and consequently strengthen the immiscibility between cholesterol and ceramide at the interface (stronger line tension along the domains enriched in ceramide and fatty acid molecules). Furthermore, such an increase in lipid density is responsible for a higher condensation of the end part of the longer alkyl chain of ceramide molecules (higher step height between the thicker and thinner phases), which, in absence of fatty acid, was most likely tilted above the (phyto)sphingosine chain that contains only 16 carbon atoms.[35]

The effect of fengycin on the nanoscale organization of the one-, two-, and three-lipid-component SC-mimicking monolayers is shown in Figure 4. Whatever the lipid composition at the air−water interface, phase separation is clearly observed in all of the images (Figure 4A,B,E,H) in the form of large, round domains (~0.7−5 μm in size) embedded in a continuous matrix that is found at a much lower step height (Table 1). Phase separation observed in mixed C_{24}-ceramide 2/fengycin (X_f = 0.25) monolayers (Figure 4A) is similar to the one found when fengycin is mixed in the same proportion and under skin physiological conditions with a C_{16}-ceramide 2.[14] Comparing our previous study with the present work, the circular shape domains observed in Figure 4A (S = 52−55% and γ = 55%) can be attributed to ceramide molecules whereas the surrounding homogeneous phase is enriched in fengycin. The domain size is not significantly influenced by the length of the fatty acid chain of the ceramides. However, as expected, this parameter considerably affects the step height values between the thicker ceramide-rich and thinner fengycin-rich phases (Δh = 0.6 and 1.2 ± 0.1 nm for ceramide/fengycin mixtures (X_f = 0.25) consisting of C_{16}-ceramide and C_{24}-ceramide species, respectively). Considering the predicted height difference between a C_{16}-ceramide and a C_{24}-ceramide (about 1.1 nm), the step height value between C_{24}-ceramide-rich and fengycin-rich phases should be about 1.7 nm instead of 1.2 nm as observed in this study. Therefore, this proves again that the C_{24}-fatty acid chain of ceramides is strongly tilted above the sphingosine chain that contains only 16 carbon atoms.

The incorporation of cholesterol into mixed ceramide/fengycin monolayers significantly decreases the step height value between thicker and thinner phases (Table 1). Moreover, this decrease in step height is dependent on the cholesterol concentration at the air−water interface. Considering the surface coverage S of thicker

(35) Abrahamsson, S.; Dahlen, B.; Löfgren, H.; Pascher, I. *Prog. Chem. Fats Other Lipids* **1978**, *16*, 125.

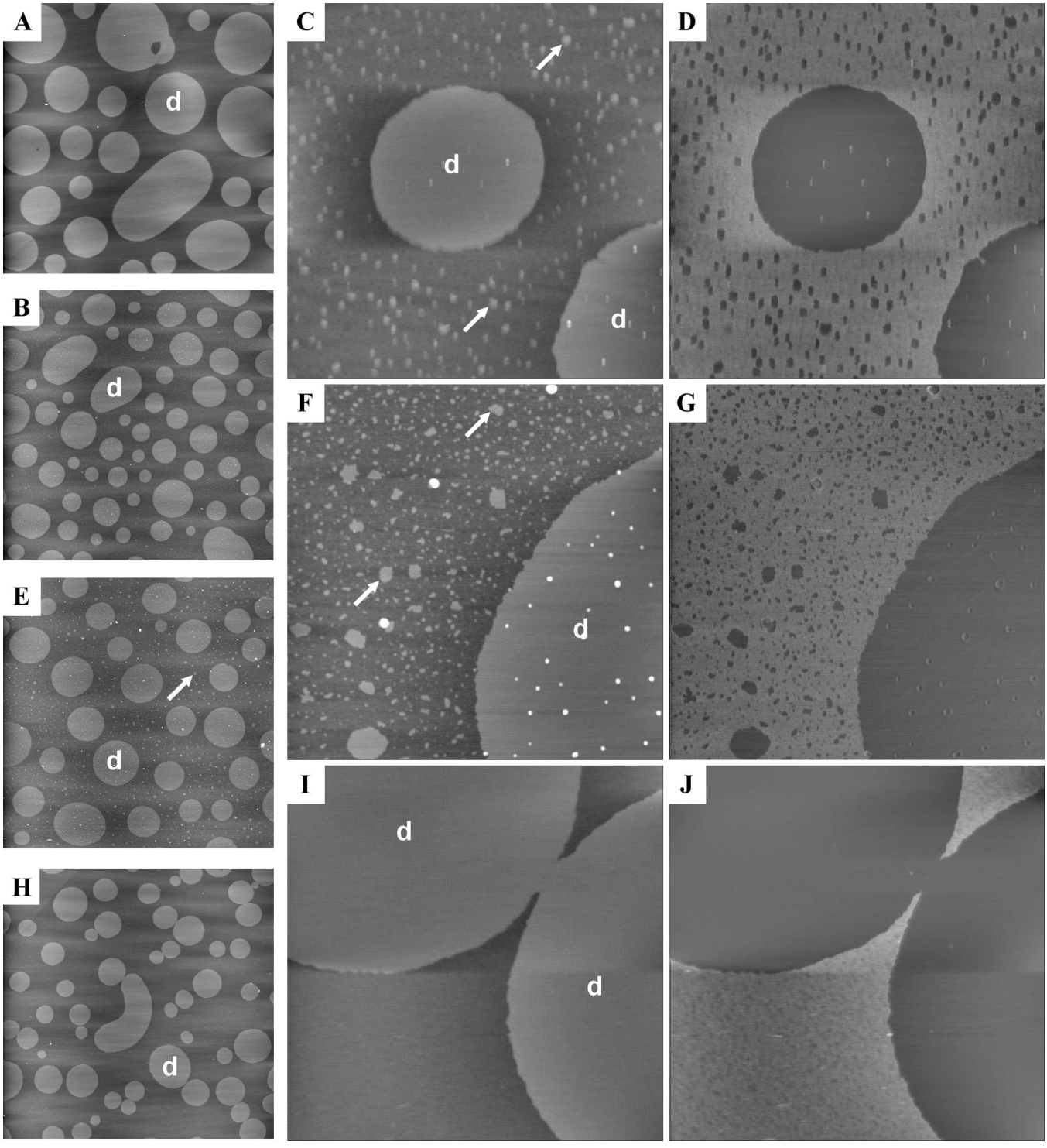

Figure 4. Effect of fengycin on the organization of SC-mimicking lipid monolayers. AFM height (A−C,E,F,H,I) (z range, 5 nm) and friction (D,G,J) (z range, 0.1 V) images (size, 20 μm × 20 μm (A,B,E,H), and 2 μm × 2 μm (C,D,F,G,I,J)) obtained for (A) mixed fengycin/ceramide (molar ratio, 0.25/0.75) monolayers; (B−D) mixed ceramide/cholesterol (molar ratio, 3/1) monolayers containing a 0.25 fengycin molar ratio; (E−G) mixed ceramide/cholesterol (molar ratio, 2/1) monolayers containing a 0.25 fengycin molar ratio; and (H−J) mixed ceramide/cholesterol/fatty acid (molar ratio: 1/1/1) monolayers containing a 0.25 fengycin molar ratio. The mixed monolayers were spread on the PBS subphase at 32 °C/pH 7.4. The surface pressure used for the LB transfer is 20 mN/m. Lighter levels in the images correspond to higher height and higher friction. Duplicate experiments using independent preparations yielded similar results. The significance of the letter "d" and the white arrows is explained in the text.

domains in the AFM images (S = 44−46% and 38−43% in Figure 4B,E, respectively) and the calculated fraction γ of the surface occupied by ceramide in the fengycin-containing monolayers (γ = 42 and 37% for monolayers of ceramide/cholesterol 3/1 and 2/1, respectively), the higher domains can be attributed to ceramide molecules whereas the surrounding phase is mainly constituted of cholesterol and fengycin. The fengycin partitioning in the cholesterol-enriched surrounding phase is confirmed by the inhomogeneous lighter level of the corresponding friction AFM images (Figure 4D,G), which denotes the presence of more than one molecular species in the lowest phase. Topographic AFM images (Figure 4C,F) focused on the lower phase of the ceramide/cholesterol/fengycin systems show that this phase contains small aggregates (noted by white arrows) that exhibit

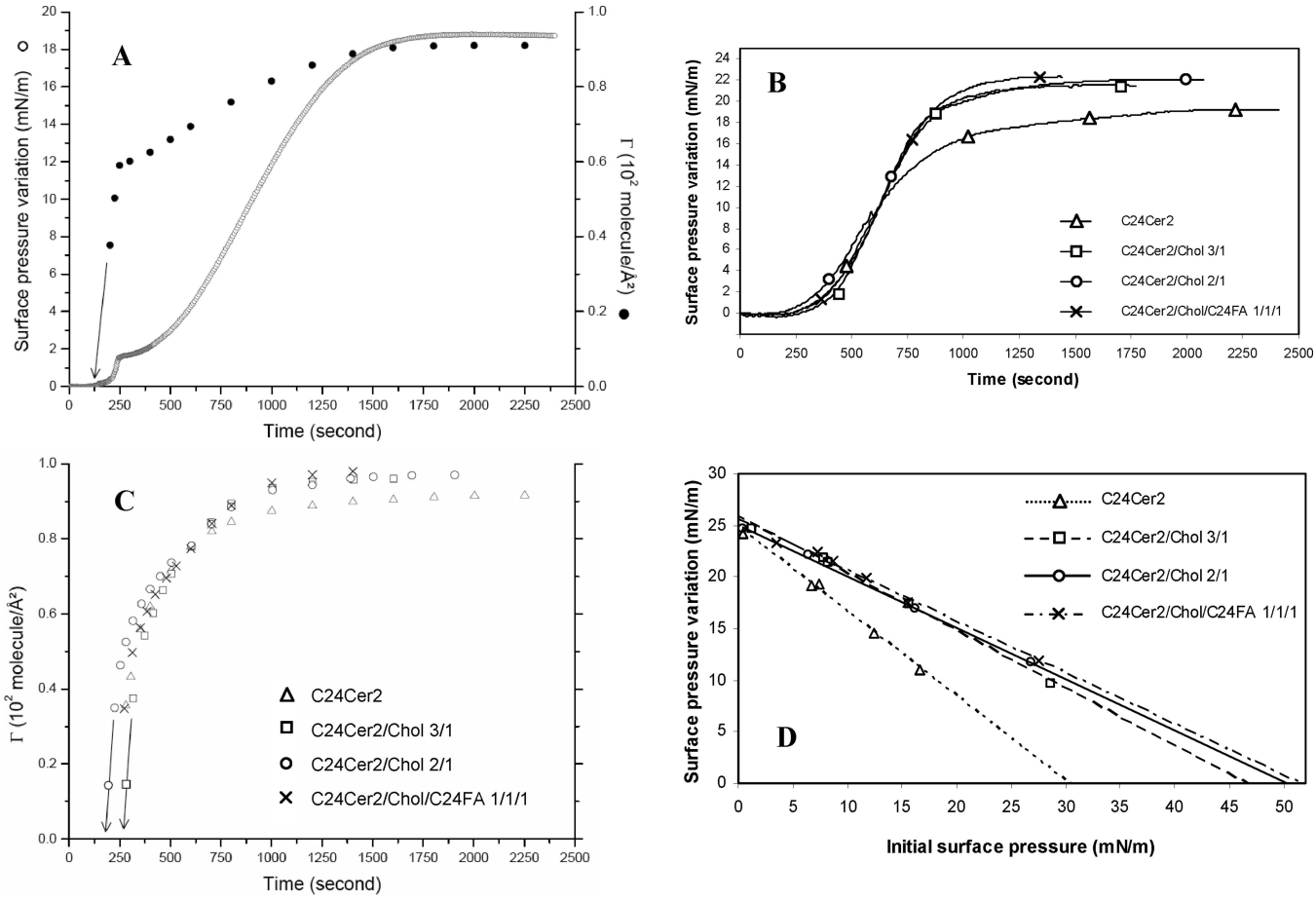

Figure 5. (A) Adsorption kinetics of fengycin following its injection into a free monolayer subphase (○) and time dependence of fengycin surface concentration Γ (●). (B) Penetration kinetics of fengycin into ceramide, mixed ceramide/cholesterol 3/1, mixed ceramide/cholesterol 2/1, and mixed ceramide/cholesterol/fatty acid 1/1/1 monolayers compressed at an initial surface pressure Π_i of about 7.5 mN/m. (C) Time dependence of fengycin surface concentration Γ following its penetration into SC-mimicking monolayers. (D) Surface pressure increase as a function of the initial surface pressure of the SC-mimicking monolayers. Subphase: PBS buffer at 32 °C/pH 7.4. Fengycin concentration in the subphase: 5.0×10^{-7} M. Injection occurs at time zero.

a step height value similar to the one between the ceramide domains (noted by "d") and their surrounding phase. In addition, these aggregates display comparable friction contrast to that of the large ceramide domains (Figure 4D,G). These two observations suggest that the small aggregates correspond to ceramides molecules that are dispersed in the continuous phase rich in both cholesterol and fengycin. The dispersion of such small ceramide aggregates does not appear to be consistent with the very smooth boundaries of the large round ceramide domains, which suggest a larger line tension at the boundaries between the ceramide domains and the cholesterol/fengycin matrix. However, as both the number and the size of small aggregates increase with the proportion of cholesterol in the system (from Figure 4B,C to Figure 4E,F), the presence of these aggregates in the surrounding phase rich in both cholesterol and fengycin may arise from the dispersal effect of excess of cholesterol that does not directly interact with fengycin.

Figure 4H−J presents topographic (Figure 4H,I) and friction (Figure 4J) images of the three-component SC-mimicking model mixed with fengycin at the air−water interface. As discussed above, the existence of strong molecular interactions between the fatty acid and ceramide molecules is responsible here for the segregation of these two components from the phase rich in both cholesterol and fengycin. The formation of thicker domains enriched in both ceramides and fatty acids is confirmed by their surface coverage S in the AFM images ($S = 31-34\%$ in Figure 4H) and the calculated fraction γ ($\gamma = 21 + 10\%$ for ceramide and fatty acid, respectively) of the surface occupied by these two components in the corresponding fengycin-containing monolayers. The enlargement of the lower phase reveals the absence of small ceramide-rich aggregates (Figure 4I) whereas they were present when no fatty acid molecules are incorporated into SC-mimicking monolayers. This further indicates that the association of fatty acid with ceramide makes it more difficult for cholesterol to disperse small ceramide aggregates. Furthermore, the corresponding friction AFM image (Figure 4J) clearly shows that the lower phase is not homogeneous, confirming that this phase mainly contains a mixture of both cholesterol and fengycin.

Penetration of Fengycin into SC-Mimicking Monolayers. Fengycin penetration experiments into the SC-mimicking monolayers were also performed in order to evaluate the effect of cholesterol and fatty acid on the insertion power of the lipopeptide into ceramide monolayers. The mixed fengycin−SC model monolayers obtained after these penetration experiments were transferred onto a mica support and analyzed by AFM to determine if the type of experiment (spread monolayers vs penetration) influences the nanoscale organization of fengycin within SC-mimicking monolayers.

Prior to the penetration of fengycin into the SC-mimicking models, the lipopeptide adsorption at a clean, lipid-free interface was evaluated. Fengycin adsorption is revealed by an increase in surface pressure as a function of time (Figure 5A, open circles). The extrapolation of the surface concentration Γ (calculated from the compression isotherm data) to a zero value (Figure 5A, solid

Table 2. Fengycin Penetration into SC-Mimicking Lipid Monolayers

SC-mimicking lipid monolayer	regression line	R^2[a]	Π_e[b]	Π_t[c]
C24Cer2	$y = -0.8185x + 24.827$	0.9968	30.3	26.7
C24Cer2/Chol 3/1	$y = -0.5574x + 25.879$	0.9968	46.4	29.6
C24Cer2/Chol 2/1	$y = -0.498x + 25.054$	0.9979	50.3	33.8
C24Cer2/Chol/C24FA 1/1/1	$y = -0.4972x + 25.595$	0.9924	51.5	31.5

[a] R^2: Determination coefficient of the regression line. [b] Π_e: Exclusion pressure (mN/m). [c] Π_t: Transfer pressure (mN/m).

circles) indicates that fengycin molecules adsorb rapidly at the air−water interface when they are injected into the bulk solution. Both the surface pressure versus time and the surface concentration Γ versus time curves exhibit a first small plateau about 250 s after the injection of fengycin into the subphase. The appearance of such a kink in both profiles may occur when the air−water interface is saturated with lipopeptide molecules in their most expanded state. This may give rise to electrostatic repulsions between fengycin molecules (which are negatively charged under our experimental conditions) already adsorbed at the air−water interface and molecules that are diffusing close to this interface. Further fengycin penetration involves a progressive rearrangement of the adsorbed lipopeptide molecules and induces an additional surface pressure increase. The maximum surface pressure variation $\Delta\Pi$ and consequently the most organized interfacial arrangement of fengycin are obtained about 30 min after its injection into the subphase ($\Delta\Pi = 18.8 \pm 0.4$ mN/m). The $\Delta\Pi$ value measured for fengycin is much lower than the value reported for surfactin ($\Delta\Pi = 36.8$ mN/m for surfactin molecules with a β-hydroxy fatty acid chain of 15 carbon atoms),[36] another lipopeptide produced by *Bacillus* strains, indicating that fengycin is a much weaker surface-active agent than surfactin.

The penetration kinetics of fengycin into SC-mimicking monolayers compressed at an initial surface pressure Π_i of about 7.5 mN/m and the related fengycin surface concentration Γ versus time profiles are shown in Figure 5B,C, respectively. The diffusion time of the lipopeptide molecules up to the interface, corresponding to the delay time before both surface pressure and surface concentration increase, is similar to that obtained in the absence of lipid monolayer. However, the presence of SC-mimicking monolayers favors the insertion of fengycin at the interface. Indeed, the absence of a kink in both the $\Delta\Pi$−time and Γ−time curves and the higher slope of the region corresponding to the linear increase in surface pressure with time indicate a faster penetration process of fengycin in the presence of a lipid interfacial film.

The plots of $\Delta\Pi$ as a function of the initial surface pressure Π_i obtained for the SC-mimicking monolayers are shown in Figure 5D. The $\Delta\Pi$ value (about 25 mN/m) measured in the presence of uncompressed SC-mimicking monolayers (i.e., for $\Pi_i = 0$ mN/m) is significantly higher than that observed for fengycin adsorption at a lipid-free air−water interface ($\Delta\Pi = 18.8 \pm 0.4$ mN/m), confirming that the adsorption of the lipopeptide is favored in the presence of SC lipids at the interface. Moreover, it can be observed that the slope of the regression lines decreases with the increase in cholesterol concentration in the ceramide-containing monolayers whereas the addition of fatty acid molecules at the interface does not further influence this parameter (Table 2). By extrapolating these regression lines to a surface pressure increase equal to zero, exclusion pressure Π_e values corresponding to the intersection with the x axis can be determined. These values reflect the penetration power of fengycin into the SC-mimicking monolayers. From the Π_e values listed in Table 2, it can be noticed that the penetration power of fengycin into SC-membrane models is much higher when cholesterol is added to a pure ceramide monolayer. It is also confirmed by the higher value of the final fengycin surface concentration (Figure 5C) under these conditions. Although the difference in slopes in Table 2 is statistically significant, the marginal effect of raising the cholesterol concentration from 25 to 33 mol% on the Π_e value appears to be rather small. Cholesterol is known for its ability to fluidize rigid bilayers[37] and has been shown in the current study to favor the dispersion of 2D ceramide domains, which consequently facilitates the insertion of fengycin into ceramide-containing monolayers. The incorporation of a C_{24}-fatty acid does not significantly affect the Π_e value.

Figure 6 presents AFM topographic images of the SC-mimicking monolayers after the penetration of fengycin. Transfer onto the solid support before AFM imaging is performed at the surface pressure corresponding to the steady-state of the fengycin penetration process (Table 2). The AFM height image observed after fengycin penetration in a pure ceramide monolayer exhibits phase separation in the form of small, irregular dark domains embedded in a gray matrix (Figure 6A). Because the step height between these two levels is similar to the one observed for a spread ceramide−fengycin monolayer ($X_f = 0.25$) (Table 1), these two phases can be attributed to fengycin-enriched domains and the ceramide matrix, respectively. A comparison of phase separation in Figure 6A with that in Figure 4A reveals the different nanoscale molecular organization of both fengycin and ceramide at the air−water interface. However, it has to be kept in mind that the surface pressure used for the transfer of the interfacial film was higher in the case of penetration experiments than in the case of spread monolayers experiments. To determine if the discrepancy in interfacial organization is due to the mechanism involved in the molecular contact between fengycin and ceramide (penetration vs spread monolayer experiments) rather than the difference in the compression state of both components in the interfacial film, the transfer of a spread ceramide/fengycin monolayer ($X_f = 0.25$) at higher surface pressure has been performed. The phase separation found at 30 mN/m (data not shown) was similar to that obtained after the penetration of fengycin into pure ceramide monolayers (Figure 6A), indicating that the interfacial organization is mainly governed by the surface pressure of the monolayers. Both the AFM height image obtained after the penetration of fengycin into a pure ceramide monolayer (Figure 6A) and that found for a spread ceramide/fengycin monolayer compressed at 30 mN/m (data not shown) exhibit smaller, lighter aggregates protruding more than 25 nm above the continuous matrix. Their regular borders and the absence of such aggregates in a spread ceramide/fengycin monolayer compressed at 20 mN/m (Figure 4A) suggest that they correspond to multilayers of fengycin squeezed out of the lipid monolayer at higher surface pressure rather than impurities.

Fengycin penetration in more complex SC-mimicking monolayers gives rise to AFM height images (Figure 6B,D,F) showing relatively different nanoscale molecular organization than that reported when fengycin is directly spread with SC models at the air−water interface (Figure 4B,E,H). Here also, differences in surface pressure values used for the LB transfer of the monolayers may be partially responsible for the discrepancy in the nanoscale organization of the components at the air−water interface. However, on the basis of the results obtained in spread fengycin/SC model monolayers, the thicker, lighter domains observed in

(36) Eeman, M.; Berquand, A.; Dufrêne, Y. F.; Paquot, M.; Dufour, S.; Deleu, M. *Langmuir* **2006**, *22*, 11337.

(37) Yeagle, P. L. *Biochim. Biophys. Acta* **1985**, *822*, 267–287.

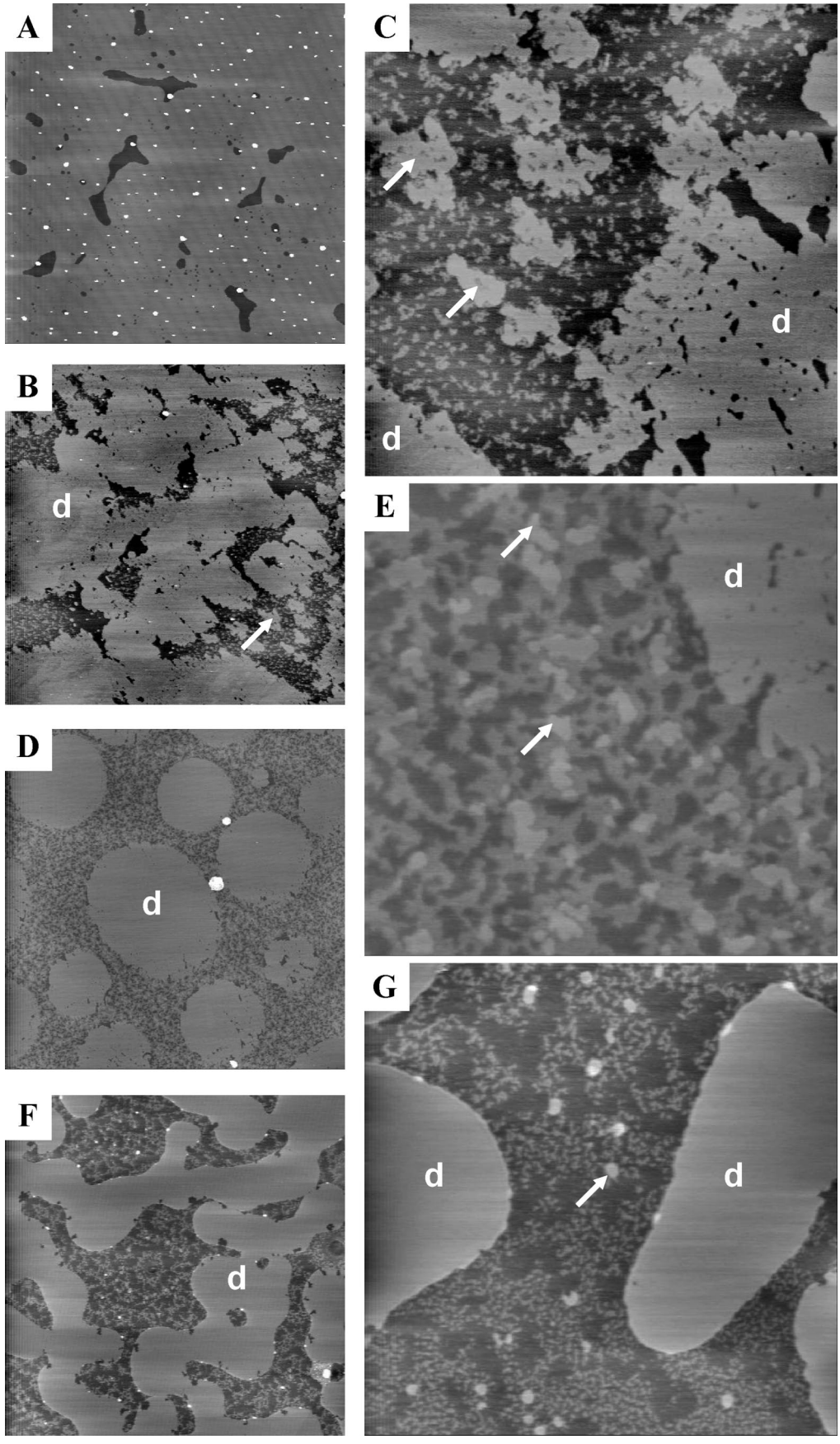

Figure 6. Effect of fengycin on the organization of SC-mimicking lipid monolayers after its penetration into the lipid interfacial film. AFM height images (sizes are 20 μm × 20 μm (A), 15 μm × 15 μm (B,D,F), 5 μm × 5 μm (C,G), and 2 μm × 2 μm (E); z range, 5 nm) obtained for (A) ceramide, (B,C) mixed ceramide/cholesterol (molar ratio, 3/1), (D,E) mixed ceramide/cholesterol (molar ratio, 2/1), and (F,G) mixed ceramide/cholesterol/fatty acid (molar ratio, 1/1/1) monolayers after the penetration of fengycin. Subphase: PBS buffer at 32 °C/pH 7.4. Surface pressure used for the LB transfer; see Table 2. Lighter levels in the images correspond to higher heights. Duplicate experiments using independent preparations yielded similar results. The significance of the letter "d" and the white arrows is explained in the text.

Figure 6B,D,F can be attributed to ceramide-enriched domains (Figure 6B,D) and to domains rich in both ceramide and fatty acid molecules (Figure 6F), respectively. The most striking difference between the AFM images obtained from the two kinds of experiments is found in the matrix surrounding these thicker domains. In the case of penetration experiments, the nonhomogeneity of the surrounding phase is accentuated, and an additional well-defined step height between the different phases can be measured (Table 1). Indeed, whatever the lipid composition of the SC models, the surrounding phase in the penetration experiments is constituted of smaller aggregates (noted by white arrows) that exhibit a similar step height value to that of the larger domains rich in ceramide or in ceramide/fatty acid molecules (noted by "d"; Figure 6C,E,G). In addition to these aggregates, the penetration AFM images also show other aggregates found at a lower level and floating on the darkest phase. On the basis of step height values observed for pure SC-mimicking monolayers, for spread fengycin/SC model monolayers, and for fengycin/SC model monolayers obtained after fengycin penetration, it is reasonable to assume that the intermediate phase in Figure 6C,E,G corresponds to domains rich in less-ordered ceramide molecules. Whatever the lipid composition of the SC models, the step height value between this phase and the lighter, thicker domains is too low to assign the intermediate phase to pure cholesterol domains. However, the presence of high proportion of cholesterol in the intermediate phase undergoing specific molecular organization with ceramide molecules is very probable. Such a hypothesis is in agreement with the work of Scheffer and colleagues who showed that cholesterol and ceramide can form a disordered, loosely packed stable phase coexisting with highly crystalline ceramide domains.[38] The darkest phase found in Figure 6C,E,G can be attributed to a mixture of both cholesterol and fengycin. The preferential partitioning of fengycin with cholesterol has already been suggested from the spread monolayer experiments.

Conclusions

The aim of this work was to investigate the influence of cholesterol and free fatty acids on the molecular interactions of fengycin with SC-mimicking lipid monolayers using a combination of AFM and the Langmuir trough technique. Two kinds of experiments were conducted: in the first one (isothem experiments), both fengycin and SC models were mixed together and spread at an air−water interface under conditions close to physiological ones (PBS subphase, pH 7.4, 32 °C). In the second kind of experiment (penetration experiments), fengycin was injected into the subphase covered with a lipid monolayer constituted of one of the four SC models used in this study.

The isotherm experiments pointed out the role of both cholesterol and fatty acid on the ability of ceramide to form 2D segregated domains at the air−water interface. Whereas cholesterol has a relatively high tendency to disperse and to reduce the size of ceramide aggregates, long-chain fatty acid molecules that are involved in very strong van der Waals interactions and hydrogen bonding with ceramide molecules are responsible for their mutual segregation from the cholesterol-rich phase. The second conclusion arising from these spread SC models/fengycin monolayers is that fengycin preferentially partitions into the cholesterol-rich phase, which surrounds the 2D domains constituted of ceramide and fatty acid molecules.

From the penetration experiments, it can also be concluded that the lipid composition of the SC models does not significantly affect the penetration kinetics of fengycin into these lipid models but strongly influences its insertion power. The presence of cholesterol facilitates the lipopeptide incorporation into the SC-mimicking monolayers. AFM measurements also indicate that fengycin preferentially partitions with cholesterol and forms a more fluid phase that is located at the lowest level. In contrast to spread fengycin/SC model monolayers, fengycin penetration into the SC-mimicking monolayers induces the formation of an additional phase found at an intermediate level that is constituted of cholesterol mixed with disordered, loosely packed ceramide molecules.

All of these results indicate that fengycin is able to modulate both the properties and the molecular organization of the three main SC lipid classes, namely, ceramides, cholesterol, and fatty acids. These observations clearly demonstrate the uptake of fengycin into cholesterol-rich regions of a monolayer but do not indicate that fengycin is able to diffuse through the extracellular lipid matrix of the SC. To investigate the potential of fengycin to overcome the physical barrier of SC, experiments involving the cell Franz-type diffusion technique and using different kinds of skin tissues (in particularly, full thickness skin and epidermal tissues) are currently in progress.

Acknowledgment. We are grateful to Professor P. Thonart and his team (Unité de Bioindustries, Faculté Universitaire des Sciences Agronomiques de Gembloux, Belgium) for the production of fengycin by the fermentation of *Bacillus subtilis* strain S499, to E. Gaigneaux for the use of the atomic force microscope, and T. Nylander for the supply of homemade devices for the Langmuir trough.

M.D. and Y.F.D. are a Research Associate and a Senior Research Associate of the National Foundation for Scientific Research (F.N.R.S.), respectively. The support of the Région Wallonne (no. EPH3310300R050F/415782) and of the FNRS is gratefully acknowledged.

LA803439N

(38) Scheffer, L.; Solomonov, I.; Weygand, M. J.; Kjaer, K.; Leiserowitz, L.; Addadi, L. *Biophys. J.* **2005**, *88*, 3381.